Article

The NorM MATE Transporter from *N. gonorrhoeae*: Insights into Drug and Ion Binding from Atomistic Molecular Dynamics Simulations

Yuk Ming Leung,[1] Daniel A. Holdbrook,[1] Thomas J. Piggot,[1] and Syma Khalid[1,*]
[1]School of Chemistry, University of Southampton, Highfield, Southampton, United Kingdom

ABSTRACT The multidrug and toxic compound extrusion transporters extrude a wide variety of substrates out of both mammalian and bacterial cells via the electrochemical gradient of protons and cations across the membrane. The substrates transported by these proteins include toxic metabolites and antimicrobial drugs. These proteins contribute to multidrug resistance in both mammalian and bacterial cells and are therefore extremely important from a biomedical perspective. Although specific residues of the protein are known to be responsible for the extrusion of solutes, mechanistic details and indeed structures of all the conformational states remain elusive. Here, we report the first, to our knowledge, simulation study of the recently resolved x-ray structure of the multidrug and toxic compound extrusion transporter, NorM from *Neisseria gonorrhoeae* (NorM_NG). Multiple, atomistic simulations of the unbound and bound forms of NorM in a phospholipid lipid bilayer allow us to identify the nature of the drug-protein/ion-protein interactions, and secondly determine how these interactions contribute to the conformational rearrangements of the protein. In particular, we identify the molecular rearrangements that occur to enable the Na^+ ion to enter the cation-binding cavity even in the presence of a bound drug molecule. These include side chain flipping of a key residue, GLU-261 from pointing toward the central cavity to pointing toward the cation binding side when bound to a Na^+ ion. Our simulations also provide support for cation binding in the drug-bound and apo states of NorM_NG.

INTRODUCTION

Bacterial multidrug transporters are membrane proteins that extrude antibiotics and other toxic compounds from within bacterial cells to the external milieu. In doing so, they play a major role in the development of bacteria that exhibit multidrug resistance, causing a serious problem for public healthcare, worldwide (1).

Multidrug transporters are divided into five main groups (2): the major facilitator superfamily (3), the small multidrug resistance family (4), the resistance nodulation cell division family, the ATP binding cassette family (5), and the multidrug and toxic compound extrusion (MATE) family. The MATE family is the latest to be identified, thus the last to be included into the multidrug efflux transporter families (6). Of the identified MATE proteins, there are only 24 that are functionally characterized and they are widely distributed in all kingdoms of living organisms, including humans, bacteria, and plants (7). The MATE transporters are secondary transport systems; they use the difference in the electrochemical potential of H^+ or Na^+ ions across the membrane to drive drug transport. Examples in humans are hMATE1 and hMATE2 transporters in which the final step in the excretion of metabolic waste and xenobiotic organic cations are carried out through electron exchange of H^+ in the kidney (8,9). In plants, MATE transporters are responsible for detoxification of secondary metabolites, including alkaloids through exchange of both Na^+ and H^+ ions (7,10), in contrast, most MATE transporters identified in bacteria, including NorM from *Vibrio cholera* (NorM_VC) (11), NorM from *Vibrio parahaemolyticus* (NorM_VP) (12), and NorM from *Neisseria gonorrhoeae* (NorM_NG) (13), export drug molecules through Na^+ ion exchange.

In this work, we focus our attention on the bacterial MATE transporter, NorM. The first x-ray structure of NorM to be determined was from *V. cholera*. It was determined at a resolution of 3.65 Å with the protein in its outward-facing ion-bound, drug-free state (Protein Data Bank (PDB) code: 3MKT). In this outward-facing conformation, a V-shaped channel is formed by transmembrane helices (TM) 1 and 8 on one side and TM 2 and 7 on the other side. As a result, the central cavity is open to the extracellular side allowing extrusion of substrate (11). Molecular dynamics (MD) simulations initiated from this structure by Vanni et. al. (14), revealed a loss in the V-shape of the NorM extracellular vestibule due to several hydrophobic residues in the outer parts of TM 1 and 2 and TM 7 and 8 forming direct interactions with each other and extruding water molecules from the lumen. As a result, water and Na^+ ions could only access the cation-binding site within

Submitted March 6, 2014, and accepted for publication June 2, 2014.

*Correspondence: s.khalid@soton.ac.uk

Daniel A. Holdbrook's present address is Bioinformatics Institute. (A*STAR), 30 Biopolis Street, #07-37 Matrix, Singapore.

Thomas J. Piggot's present address is Detection Department, Defence Science and Technology Laboratory, Porton Down, Salisbury, Wiltshire, SP4 0JQ.

Editor: Nathan Baker.

0006-3495/14/07/0460/9 $2.00

http://dx.doi.org/10.1016/j.bpj.2014.06.005

the protein through a narrow permeation pathway. In addition, they also suggested that there are two distinct modes of Na^+ ion binding (competitive and simultaneous) in the cation-binding site, which could be crucial for inducing the conformational change from the outward-facing to the inward-facing state. The loss of the vestibule V-shape was also reported from a similar MD study by Song et al. (15). Interestingly, in contrast to Vanni et al., the authors of this study suggested that two Na^+ ions bind to the cation-binding site of NorM_VC.

Recently, four x-ray structures of NorM_NG (from *N. gonorrhoeae*) have been determined. All of the structures have a resolution of ~3.6 Å and capture the protein in its outward-facing conformation with a drug molecule, tetraphenylphosphonium (TPP) present in the central cavity of the protein (PDB codes: 4HUK, 4HUM, and 4HUN). One of the structures also reveals a Na^+ ion present in the cation-binding site (PDB code: 4HUL) (16). Interestingly, superimposition of the NorM_VC x-ray structure, which represents a cation-bound and drug-free state, with the NorM_NG crystal structure (drug-bound and cation-free state), revealed that helices TM 7 and TM 8 moved ~0.6 nm away from the central cavity, toward helix TM 10 (16). It has been hypothesized that the binding of Na^+ to the cation-binding site, which is located at the C-terminal end of the protein, and is formed by residues GLU-261, TYR-294, and ASP-377 from TM7, TM8, and TM10, respectively, could play a role in this conformational rearrangement of the TM helices. These structures combined with the NorM_VC structures enabled Lu et. al. (16) to propose an antiport mechanism of transport, in which there are six distinct states; three in each of the outward-facing and inward-facing conformations.

They proposed that initially the protein in its outward-facing, drug-bound, ion-free state (PDB codes: 4HUK, 4HUM, and 4HUN) takes in Na^+ ions from the extracellular side, mediated by residues GLU-261 and TYR-294. Once the Na^+ ion is in the cation-binding site (as in the structure PDB code: 4HUL), a conformational change occurs. TM7 and TM8 move toward TM10, which in turn enables residue ASP-377 to form an electrostatic interaction with the Na^+ ion. This conformational rearrangement results in disruption of protein-drug interactions, specifically those involving residues PHE-265, GLN-284, and SER-288. This triggers the extrusion of the bound drug into the periplasmic space. After the drug is extruded, the ion-bound, drug-free transporter (3MKT) undergoes a more substantial conformational rearrangement, to the inward-facing state, from which it can capture another drug molecule. Upon drug binding, TM7 and TM8 move back to the central cavity, followed by release of the Na^+ ion from the binding site into the cytoplasm. The drug-bound, ion-free transporter then rearranges into the outward-facing conformation that completes the mechanistic cycle.

Despite the clearly plausible and elegant mechanism put forward by Lu et al., the structures of NorM_NG do raise some questions concerning the outward-facing phase of the proposed antiport mechanism. First, the presence of the drug molecule in the central cavity of the transporter may provide an obstacle for the passage of the Na^+ ion into the cation-binding site. A previous simulation study showed the Na^+ ion moves into the binding site through a narrow permeation pathway without the drug molecule present in the central cavity (14). Thus, the effect of the drug on ion binding is still unresolved. Second, although the x-ray structures reveal specific conformation states that comprise the transport cycle of the antiport mechanism, the precise conformational rearrangement events that provide the transitions between these states, remain elusive.

From a mechanistic perspective, characterizing the dynamics of the protein are important in identifying any conformational changes that may occur to enable cation binding. In particular, in terms of the mechanism proposed earlier, we may ask are cations able to bind after the drug-binding event? This would provide further support for the idea that cation-binding triggers drug extrusion.

To address these questions, we have carried out multiple atomistic molecular dynamics simulations of the NorM_NG transporter in a palmitoyloleoylphosphatidylcholine (POPC) lipid bilayer. Our results provide molecular-level details of drug and ion binding to NorM_NG. Moreover, our simulations provide further evidence for the proposed antiport mechanism in which the ion-binding event leads to drug extrusion from the outward-facing state of the protein in the final phase of the transport cycle.

MATERIALS AND METHODS

The x-ray structure was obtained from the PDB with the PDB code 4HUK (16). Parameters for the TPP drug were obtained using automated topology builder (17). The protein-drug complex was embedded into a POPC lipid bilayer using the GROMACS utility g_membed (18).

Atomistic simulations were performed using GROMACS version 4.5.1 (19–21). The simulations used the united-atom GROMOS 54A7 force field (22) with POPC lipids adapted from the Berger parameters (23). Water molecules were treated explicitly using the SPC water model (24). 502 POPC lipids, 30,739 water molecules were present in the simulation systems with a simulation box size of 12.5 × 12.5 × 10 nm in the *x*, *y*, and *z* dimensions, respectively. The equivalent of 100 mM of sodium and chloride ions were added to the simulation systems. Additional ions were added to ensure all systems were charge neutral. Ionizable side chains were modeled in their default states at neutral pH. All lipid and protein bonds were constrained using the LINCS algorithm (25) and waters were constrained using the SETTLE algorithm (26), allowing for a time step of 2 fs to be used. Energy minimization was performed using the steepest descent algorithm for 1000 steps to remove any overlapping contacts. Position restraints with 1000 kJ mol^{-1} nm^{-2} were applied to the C_α of the protein for the first 10 ns of certain simulations (see Table 1) to allow a reequilibration of the solvent around the protein. The Nosé-Hoover thermostat, with a time constant for the coupling of 0.5 ps, was used to maintain the system temperature at 298 K (27). The Parrinello-Rahman barostat, with a time constant of 5.0 ps, was used to maintain the system pressure at 1.0 bar (28). Electrostatic interactions used a cut-off of 1 nm

TABLE 1 Table of all the simulations performed

Simulation	Simulation time (nanosecond)	First 10 ns with RES[a]	Drug present in central cavity of protein	100 mM NaCl present in bulk of system
unbound_v1	210	Yes	No	No
unbound_v2	210	Yes	No	No
unbound_v3	210	Yes	No	No
bound_v1	210	Yes	Yes	No
bound_v2	210	Yes	Yes	No
bound_v3	210	Yes	Yes	No
unbound_ion_v1	210	Yes	No	Yes
unbound_ion_v2	210	Yes	No	Yes
unbound_ion_v3	210	Yes	No	Yes
bound_ion_v1	500	Yes	Yes	Yes
bound_ion_v2	500	Yes	Yes	Yes
bound_ion_v3	500	Yes	Yes	Yes
bound_ion_v4	200	No	Yes	Yes
bound_ion_v5	200	No	Yes	Yes
bound_ion_v6	200	No	Yes	Yes
bound_two_ion_v1	500	Yes	Yes	Yes
bound_two_ion_v2	200	Yes	Yes	Yes
bound_two_ion_v3	200	Yes	Yes	Yes
ProtE261_D377_v1	210	Yes	No	Yes
ProtE261_D377_v2	210	Yes	No	Yes
ProtE261_D377_v3	210	Yes	No	Yes
Mutant_D41A_v1	210	Yes	No	Yes
Mutant_D41A_v2	210	Yes	No	Yes
Mutant_D41A_v3	210	Yes	No	Yes

[a]Positional restraints were applied on the C_α atoms of the protein for the first 10 ns.

with interactions beyond this cutoff treated using the smooth particle mesh Ewald method (29). The van der Waals interactions also used a cut-off of 1 nm with a long-range dispersion correction applied for the energy and pressure. The neighbor list was updated every 5 steps. The components of all the simulations are summarized in Table 1. All the simulations were performed on the Iridis-4 supercomputer at the University of Southampton. DSSP and GROMACS tools were used to determine the conformation properties of the NorM_NG (30). Visualization of simulation trajectories was conducted in VMD (31). An additional set of simulations was performed to study the effect of the charge state of residues GLU-261 and ASP-377, where ProtE261_D377v1-3 refer to simulations in which both GLU-261 and ASP-377 are protonated. Finally, the D41A mutant was also simulated (Mutant_D41Av1-3), given experimental data showed this mutant completely abolished transport activity (16). Three independent simulations of each protonated system and the mutant were performed.

RESULTS AND DISCUSSION

Structural drift and fluctuations

To evaluate the conformational stability of the protein structure on the timescale of the simulations, the structural drift was measured via calculation of the root mean-square deviation (RMSD) from the initial starting structure of NorM_NG over multiple simulations. In all of the simulations, the RMSD values reached a plateau value between ~50 to 100 ns. In general, the greatest deviation was observed in loops 3–4 and 9–10, although the most stable secondary structural elements were the TM helices 1–12 (Figs. S1–S3 in the Supporting Material). Specifically, in all three sets of simulations, loops 3–4, 6–7, and 9–10, had plateau RMSD values of ~0.5 nm after 20 ns, whereas the RMSD of the other loops and helices TM1-12 remained at ~0.2–0.3 nm throughout the 200 ns simulation (Figs. S1–S3). These large variations in the RMSDs between loops 3–4, 6–7, and 9–10 and the other loops indicate a greater degree of flexibility in the former. Block analysis (32) of the RMSD values over the final 50 ns of the simulations showed that the standard error of the mean converged for block sizes of >20 ns, indicating converged trajectories (Fig. S4). Encouragingly, a previous MD simulation study suggested that loops 3–4 and 9–10 are likely to play an important role in the process of drug extrusion (16).

After position restraints were removed from the protein, we observed partial collapse of the V-shape extracellular vestibule of NorM_NG, in agreement with the two previous simulation studies of NorM_VC (14,15) (Fig. 1). Furthermore, analysis of the all-to-all RMSDs of the protein revealed that even after 210 ns of simulation, the overall three-dimensional architecture of the protein continued to undergo conformational drift (Fig. S5), suggesting there may be more than one energetically favored state. In further support of this hypothesis, simulations of NorM_VC (multiple repeats including simulations using a different force field for lengths of up to 1 μs; see the Supporting Material for more information) also revealed the continued increase in protein conformational drift (Fig. S6).

To explore these changes in conformation of the NorM_NG protein, the stability of the secondary structure

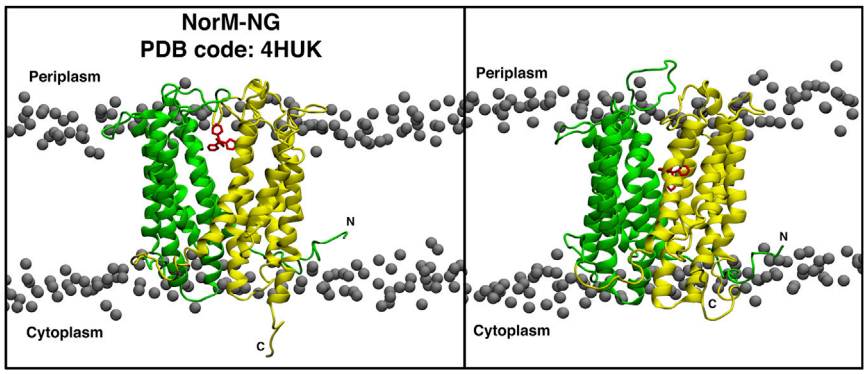

FIGURE 1 Snapshot of the simulation system before the equilibration step (*left*) shows the x-ray structure of the protein, NorM-NG, and the drug molecule, TPP, embedded in a POPC bilayer. The system after 500 ns of simulation is shown in the panel on the right. The amino (1–6 TM helices) and carboxyl (7–12 TM helices) terminal domains of the protein are colored green and yellow, respectively. TPP is colored in red. The letters "N" and "C" indicate the amino and carboxyl terminal of the protein. The gray spheres indicate the POPC lipid headgroups. Water and ions in the system are omitted for clarity. To see this figure in color, go online.

was evaluated using the DSSP analysis code (30). Encouragingly, results showed all of the TMs retained their α-helical conformation throughout the simulations (Fig. 1 and Fig, S7). Having established the stability of the protein secondary structure on the timescale of the simulations, we sought to investigate the interactions between the drug and ion with the protein to gain insight into the role they play in this outward-facing phase of the proposed mechanism. However, before the investigation of these interactions, we performed additional analysis to ascertain if there were any conformational rearrangements of the region of the protein implicated in drug and ion binding (see Table S1) (16). RMSD analysis (including all-to-all RMSDs) of this region revealed that these regions were not subject to structural drift over the timescale of the simulations (Fig. S5). This provided confidence that the continued changes in protein conformation were not impacting upon the observed drug and ion interactions.

Movement of Na^+ ion

X-ray structures of the outward-facing conformation of NorM transporters reveal a monovalent cation-binding site in the protein. Given that NorM transporters exploit either a Na^+ or H^+ gradient across the membrane to drive substrate export, to determine the sequence of events in the transport process we may ask if ions are able to enter the cation-binding site once the drug is bound. Experimental evidence indicates this may be the case; x-ray structures from the apo-NorM crystals soaked in solution containing Cs^+ (Na^+ analog) revealed a Cs^+ binding site located outside the drug-binding cavity. Of importance, the x-ray structure did not show significant conformational deviation from the cation-free, TPP-bound NorM_NG structure (RMS deviation of 0.05 nm), used to initiate our simulations (16). To explore the movement of Na^+ once TPP is already bound the center of mass motion of Na^+ ions was monitored throughout the simulations (Fig. 2). It is worth reiterating here that the equivalent of 100 mM of NaCl ions were added to certain simulation systems (see Table1). In general, we observe a pathway through the protein to the cation-binding site that is lined by aspartate residues, specifically residues ASP-52, ASP-355, ASP-356, and ASP-41. The Na^+ ion initially binds (where bind is defined as a protein-ion distance of $\leq$0.3 nm) to ASP-52 in loop L1-2, subsequently it rapidly (within 1 ns) moves toward residues ASP-355, ASP-356, and then ASP-41, where it associates with each one in turn before entering the cation-binding site (Fig. 2 and Fig. S8).

In all three simulations unbound_ion_v1-3 (no TPP) during the first 10 nanoseconds of the simulation, while the C_α of the protein is still subjected to positional restraints, a single Na^+ ion was observed to move into the cation-binding site, through the previously described aspartate pathway, in agreement with a similar computational study (14). In contrast, in simulations bound_ion_v1–6 (in which TPP is present), a Na^+ ion moved into the cation-binding site in two out of the six simulations (bound_ion_v2 and v3). In the other four simulations, the TPP molecule appears to physically obstruct movement of Na^+ into the cation-binding site. In all of our six simulations, whether the Na^+ ion ended up moving into the cation-binding site or not, we observed the ion first bound to ASP-41 before entering the central cavity, indeed the presence of TPP appears to guide movement of the ion toward ASP-41 (Fig. 3).

The Na^+ ion remained within 0.3 nm of ASP-41 for over 5 ns in simulation bound_ion_v1 and v3. In simulation bound_ion_v2, Na^+ ion moved away from ASP-41 as it moved into the cation-binding site after 3 ns. In the same simulation, as a Na^+ ion approached the cation-binding site it interacted with residue GLU-261. The side chain of residue GLU-261 was initially pointing toward the central cavity, however upon interaction with the Na^+ ion, it flipped toward the cation-binding site, thereby facilitating the movement of the ion associated with it, into the binding site. Within one nanosecond of entering the cation-binding site, the ion interacted with residues TYR-294 and ASP-377, although still being bound to GLU-261 (Fig. 2). We also observed flipping of the GLU-261 side chain, and interactions with TYR-294 and ASP-377 in simulations unbound_ion_v1 to v3 when the ion moves into the binding site. Of importance, in simulations (bound_ion_v1 and bound_v1-6) in which Na^+ does not bind, flipping of GLU-261 toward the cation-binding site is not observed (Fig. 4). However, there is some flexibility of the side chain such that it deviates slightly from the x-ray structure. To further investigate the importance of the specific protein-cation interactions, we studied NorM_NG in an additional ionization state; with GLU-261 and ASP-377 both protonated (rather than charged) in three independent simulations (ProtE261_D377v1-3). In all three simulations a Na^+ ion was observed to enter the central cavity of the protein. However, the Na^+ ion was not observed to move into the cation-binding site in any of these simulations. In fact, in two of the three simulations (v2 and v3), the Na^+ ion moved out of the central cavity and subsequently exited the protein completely after ~40 and ~20 ns, respectively. Encouragingly, experimental studies have indicated that these residues are responsible for binding and stabilizing the ion in the binding site; Lu et al. showed that NorM_NG mutants E261A and Y294L were unable to decrease the sensitivity of the bacterium toward drugs like ethidium and TPP. This was hypothesized to be most likely due to the loss of the transport function of the protein (16). In another mutational study of the NorM_VC D371N (equivalent to ASP-377 of NorM_NG), the binding of Na^+ was completely abolished (11). In addition, mutations to GLU-261, in NorM_VP GLU-251, and hMATE1 GLU-273 also inhibited substrate transport activity (8,33,34).

To investigate the importance of ASP-41, we performed three independent simulations of the D41A mutant

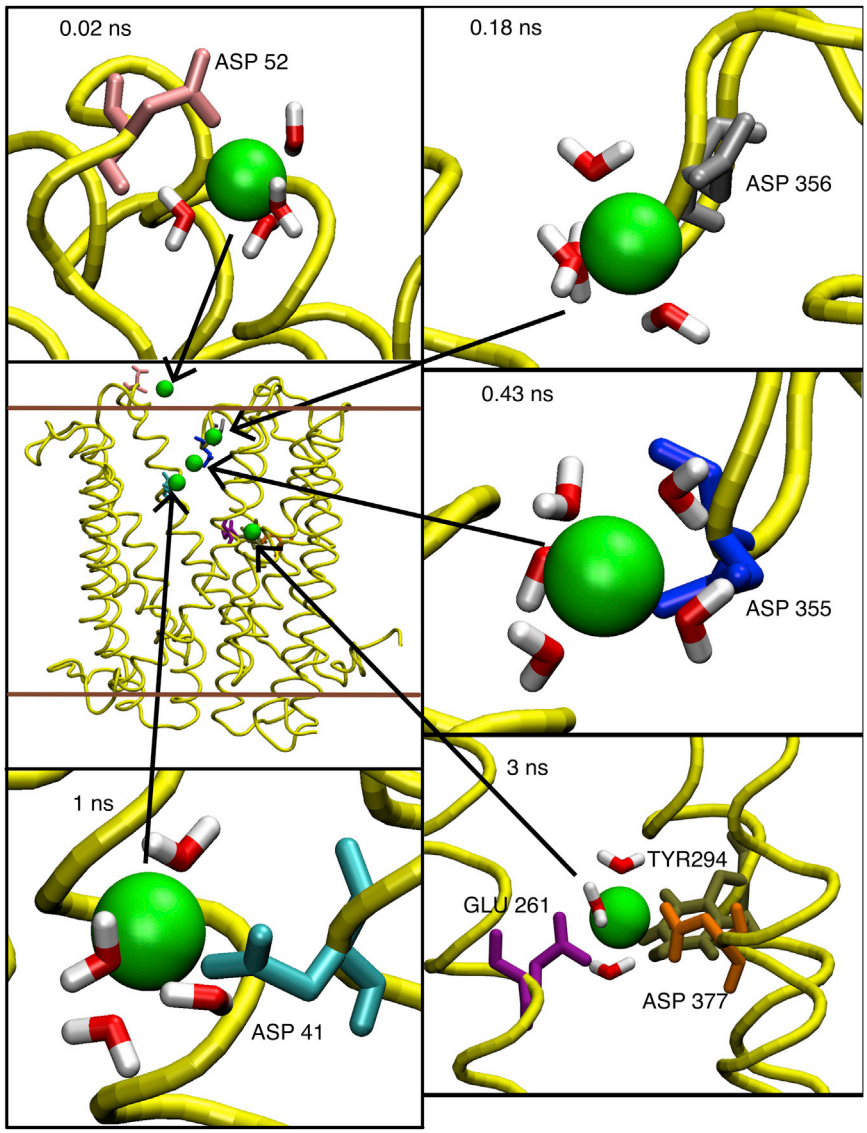

FIGURE 2 The middle panel of the left column shows five stages of the movement of the Na^+ ion within the first 10 ns of bound_ion_v2 simulation. The Na^+ ion moves into the central cavity and subsequently the cation-binding site from the extracellular space, via a pathway that involves electrostatic interactions with five different ASP residues. The other panels show close-up views of specific Na^+- ASP interactions. Water molecules within 0.3 nm of the ion are also shown. The simulation times at which the snapshots are extracted are stated at the top left corner of the panels. The protein is yellow, Na^+ ion is green, ASP-52 is pink, ASP-356 is gray, ASP-355 is blue, ASP-41 is cyan, GLU-261 is purple, TYR-294 is tan, ASP-377 is orange, and water is red and white. The brown lines indicate the lipid headgroups. Part of TM2 and loop 3 and 4 of the protein, lipid tails, other water molecules, and ions in the system are omitted for clarity. To see this figure in color, go online.

(Mutant_D41A_v1-3). In two out of three simulations (v1 and v3), not a single Na^+ ion is observed to bind in the cation-binding site. In v1 a Na^+ ion was observed to move into the central cavity of the protein, after which it subsequently oscillated between the central cavity and cation-binding site, never remaining in the cation-binding site for >10 ns at a time. In v3, the Na^+ ion moved out of the protein in the first 10 ns of the simulation, and no other Na^+ ion was observed to enter the central cavity of the protein during the remainder of the simulation. In contrast, in simulation v2, a single Na^+ ion was observed to move into the cation-binding site via GLU-261 and remained in the site forming interactions with GLU-261, TYR-294, and ASP-377 throughout the remaining 200 ns of simulation. Taken together, these simulation results suggest a reduced affinity for Na^+ ions when ASP-41 is mutated. Previous experimental mutational studies have reported the efflux activity of NorM_NG toward the drug molecule Rhodamine 6G, which is completely abolished in D41A. Based on the experimental observations, our simulations and the previously proposed mechanisms of drug extrusion, we hypothesize that the molecular origins of abolition of drug transport activity in D41A may be that the disruption of the interactions between residues on TM 7 (PHE-265) and 8 (SER-288), and the drug molecule, that lead to drug extrusion in the wild-type protein are inhibited in the low cation-affinity mutant.

Water molecules in the binding site provide additional stabilizing interactions with the Na^+ ion. In the unbound protein, ~50 water molecules move into the interior of the protein, from the extracellular side within the first 2 ns of the simulation. Approximately 40 of the water molecules are located within the central cavity, and 10 or so are in the cation-binding site. Within the cation-binding site,

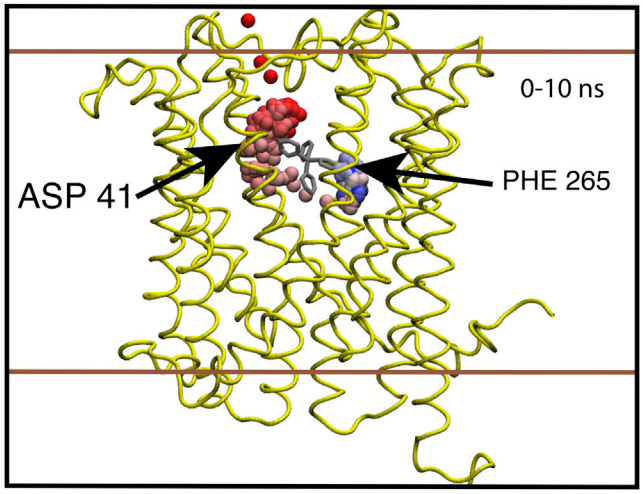

FIGURE 3 The Na^+ ion moves readily into the cation-binding site via the central cavity. Figure shows the movement of the Na^+ ion into the cation-binding site. The spheres represent the location of the ion during the first 10 ns of simulation bound_ion_v2. Red, white, blue color scheme is used, red is at the start of the simulation, and blue is at time = 10 ns. The protein backbone is shown in tube representation and is colored yellow. The drug is shown in gray. The brown lines indicate the lipid headgroups. Lipids, water, and other ions in the system are omitted for clarity. To see this figure in color, go online.

although the Na^+ is bound to residues GLU-261, TYR-294, and ASP-377 as described previously, it is also coordinated by 2–4 water molecules (Fig. 2). Interestingly, even in the presence of the drug molecule, TPP, a similar number of water molecules were observed to enter the protein interior as the unbound simulations, with stabilization of the Na^+ through a combination of interactions with the protein and water molecules. The results presented here not only provide further support for the functional relevance of the cation-binding site of NorM_NG (11,16,33) but also reveal the molecular-level details of the dynamics of the interplay between the protein residues, water molecules, and the Na^+ ion. Our hypothesis is that GLU-261 is the residue responsible for bringing Na^+ ions into the cation-binding site from the central cavity, whereas TYR-294, ASP-377, and water molecules provide stabilizing interactions that anchor the cation within the binding site.

The drug may play a role in binding and stabilization of the ion within the cation-binding site

Given we do observe a Na^+ ion entering the cation-binding site, even in the presence of the bound drug molecule (in two out of six simulations, specifically bound_ion_v2 and bound_ion_v3), we may ask if the drug plays a role in stabilizing/destabilizing the ion. To explore this, we have examined the molecular processes that occur subsequent to the ASP-41-Na^+ binding event. The drug molecule, TPP binds to PHE-265 (in TM7) within 1 ns of the start of the simulations (Fig. S9). In doing so, the TPP moves ~0.2 nm toward the central cavity of the protein, in particular toward TM7, from its initial position in the x-ray structure (Fig. 3). This movement of the drug toward TM7 seems to be a key step for Na^+ movement into the cation-binding site. Although the TPP molecule is in its original position as in the x-ray structure, it prevents interaction of the Na^+ and GLU-261.

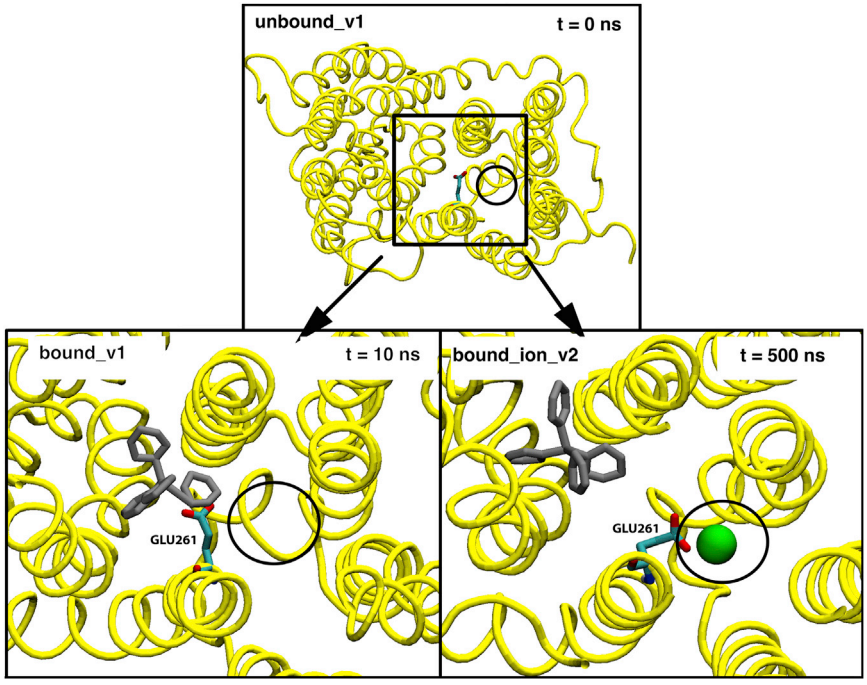

FIGURE 4 Snapshots showing the change in the orientation of the side chain of GLU-261. The panel on the top shows the position of GLU-261 in apo NorM_NG. The black circles correspond to the approximate position of the cation-binding site. The panel on the bottom left is a zoomed in view of GLU-261 from simulation bound_v1. The bottom right panel is taken from the bound_ion_v2 simulation, showing the side chain of GLU-261 pointing toward the cation-binding site with a Na^+ ion present in the cation-binding site. The protein is shown in a yellow tube representation, GLU-261 is shown in a sticks representation, Na^+ ion is green, and TPP gray. Water molecules, lipids, and other ions are omitted for clarity. To see this figure in color, go online.

Once it has moved closer to TM7, an unobstructed pathway from the solvent to the cation-binding site is created, enabling the Na^+ to interact with the side chain of GLU-261 and subsequently move past the drug, into the binding site.

In simulations unbound_ion_v1-3, in which TPP was not present, Na^+ ion moved into the cation-binding site during the first 10 ns of the simulation. In these simulations after the initial binding of the Na^+ ion within the cation-binding site, it was observed to move in and out of the this site throughout the course of simulation. Whereas in simulation bound_ion_v2 and v3, after the ion was bound within the binding site, it remained in the site more readily than observed in the absence of drug in the unbound_ion simulations. In the transport mechanism stated from previous experimental study by Lu and co-workers (16), the drug would be present when Na^+ ion moved into the cation-binding site, and it is the binding of Na^+ ion to the binding site that causes drug extrusion by disrupting interactions between the drug and TM 7 and 8 of the protein. In addition, in simulation bound_ion_v2, the drug moved slightly away from PHE-265 after the ion bound to the binding site (Fig. S9), to be positioned more centrally in the central cavity. From this observation, it seems that there is a possibility that the drug could play a role in ion stabilization by obstructing the pathway leading away from the binding site.

Two Na^+ ion binding mode of NorM

Previously, a binding mode in which two Na^+ ions occupy the cation-binding site of NorM_VC has been proposed (15). MD simulations indicated that this two-ion-binding might contribute to the induced conformational change of NorM_VC from the outward-facing to the inward-facing conformation. In all of our unbound_ion and bound_ion simulations, only one Na^+ ion is present at any given time, within the binding site. Whereas in the bound_ion_v1 simulation, physical obstruction by the drug, prevented even one ion entering the cation-binding site. To explore the possibility of two Na^+ ions occupying the cation-binding site in NorM_NG, we performed three additional simulations, this time with two ions in the cation-binding site. A system snapshot was extracted after 10 ns from the bound_ion v2 simulation and a second ion was manually placed within the cation-binding site. Three independent simulations of this system revealed that only one ion remains permanently within the binding site. The second ion was observed to move away from the binding site after 5–20 ns, and out of the protein completely into the bulk solvent after ~80 ns. Interestingly, the presence of the drug did not prevent the movement of the ion into, or out of the cation-binding site, in other words it did not obstruct the path of the ion. The single remaining Na^+ ion occupied the binding site throughout the remainder of the respective simulations. For comparative analysis of the ion dynamics of MATE transporters, we also performed simulations of the x-ray structure of NorM_VC, PDB code 3MKT (see Table S2). In each of the three simulations, we observed one Na^+ ion entering the cation-binding site during the equilibration stage of simulation. In two of the simulations, a second Na^+ ion was observed to enter the binding site from the central cavity after further ~35 and ~100 ns, respectively. The two ions simultaneously occupied the binding site for between ~2 and 5 ns, after which one ion moved out (Fig. 5). In one of the two-ion-binding simulations, another ion was observed to enter the central cavity after ~10 ns of the initial two-ion-binding event, from where it subsequently moved into the cation-binding site. This second two-ion-binding state was short-lived; lasting only ~0.5 ns, after which one Na^+ ion was extruded. The previous observations are in qualitative agreement with previous simulation studies of this protein and suggest that the two-ion-binding mode does exist in NorM_VC and may be an intermediate state with a possible role in TM helix

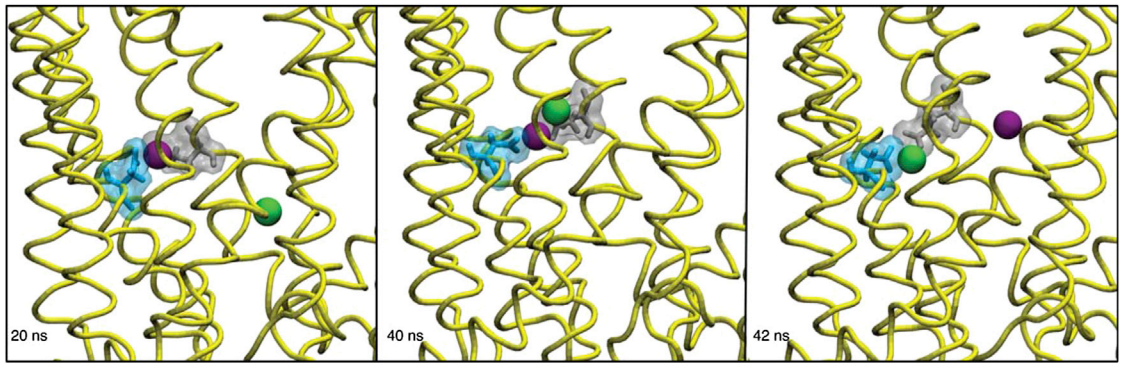

FIGURE 5 Three snapshots taken from simulation 3MKT_apo_v1 showing the competitive binding of two Na^+ ions. The panel on the left shows a Na^+ ion (*purple*) interacting with GLU-255 (*silver*) and ASP-371 (*cyan*) in the cation-binding site, and another Na^+ ion (*green*) in the central cavity of the protein at 20 ns of the simulation. The panel in the middle shows the Na^+ ion, which was originally in the central cavity, having also moved into the cation-binding site. The cation-binding site contains two-ions at this point (~40 ns). The panel on the right shows that after a further ~2 ns the Na^+ ion that was initially in the cation-binding site, is extruded into the central cavity. To see this figure in color, go online.

rearrangements that lead to conformational change of NorM (15). In contrast, the evidence for a two-ion-binding state is less convincing for NorM_NG, and if it does exist, it is likely to be very short-lived.

It is important to consider the methodological limitations of the current studies. Perhaps the primary limitation of the simulations is the relatively short duration (>200 ns) of the MD calculations. Longer simulations would improve the sampling of the protein conformational dynamics. However, to some extent we have addressed this by performing multiple simulations of each system. Despite this limitation, the current study is encouraging in that it enables the rationalization of experimental observations and shows that conventional atomistic simulations may be applied to identify solute permeation pathways through membrane proteins, and indeed in this case allows us to propose one part of a transport mechanism (Fig. 6).

CONCLUSIONS

In conclusion, we have identified the pathway taken by a monovalent cation to enter the cation-binding site of NorM_NG, and the key intermolecular interactions that stabilize this ion within the binding site. We have shown that the presence of a bound drug molecule does not prevent movement of the ion into the binding site, but may in fact even stabilize it. The stabilization of the ion in the binding site is likely to cause the protein to proceed to the drug extrusion stage. Our simulations suggest that a two-ion binding state is more likely in NorM_VC than NorM_NG. Thus, our simulation study has added some of the hitherto missing pieces of the puzzle represented by the mechanism of the NorM transport cycle. It is important to note that future extensions of the current study would involve consideration of a membrane model that better mimics the in vivo environment of NorM_NG, both in terms of lipid content and the crowded protein environment, indeed such complex membrane models have already been reported for eukaryotic (35) and prokaryotic organisms (36,37).

SUPPORTING MATERIAL

Nine figures, two tables, and supporting data are available at http://www.biophysj.org/biophysj/supplemental/S0006-3495(14)00607-9.

The authors acknowledge the use of the Iridis-4 supercomputing facility at the University of Southampton and the input of various members of the Khalid group.

REFERENCES

1. Fischbach, M. A., and C. T. Walsh. 2009. Antibiotics for emerging pathogens. *Science.* 325:1089–1093.
2. Putman, M., H. W. van Veen, and W. N. Konings. 2000. Molecular properties of bacterial multidrug transporters. *Microbiol. Mol. Biol. Rev.* 64:672–693.
3. Pao, S. S., I. T. Paulsen, and M. H. Saier, Jr. 1998. Major facilitator superfamily. *Microbiol. Mol. Biol. Rev.* 62:1–34.
4. Bay, D. C., K. L. Rommens, and R. J. Turner. 2008. Small multidrug resistance proteins: a multidrug transporter family that continues to grow. *Biochim. Biophys. Acta.* 1778:1814–1838.
5. Fath, M. J., and R. Kolter. 1993. ABC transporters: bacterial exporters. *Microbiol. Rev.* 57:995–1017.
6. Brown, M. H., I. T. Paulsen, and R. A. Skurray. 1999. The multidrug efflux protein NorM is a prototype of a new family of transporters. *Mol. Microbiol.* 31:394–395.
7. Omote, H., M. Hiasa, …, Y. Moriyama. 2006. The MATE proteins as fundamental transporters of metabolic and xenobiotic organic cations. *Trends Pharmacol. Sci.* 27:587–593.
8. Otsuka, M., T. Matsumoto, …, Y. Moriyama. 2005. A human transporter protein that mediates the final excretion step for toxic organic cations. *Proc. Natl. Acad. Sci. USA.* 102:17923–17928.
9. Masuda, S., T. Terada, …, K. Inui. 2006. Identification and functional characterization of a new human kidney-specific H+/organic cation antiporter, kidney-specific multidrug and toxin extrusion 2. *J. Am. Soc. Nephrol.* 17:2127–2135.
10. Otani, M., N. Shitan, …, K. Yazaki. 2005. Characterization of vacuolar transport of the endogenous alkaloid berberine in *Coptis japonica*. *Plant Physiol.* 138:1939–1946.

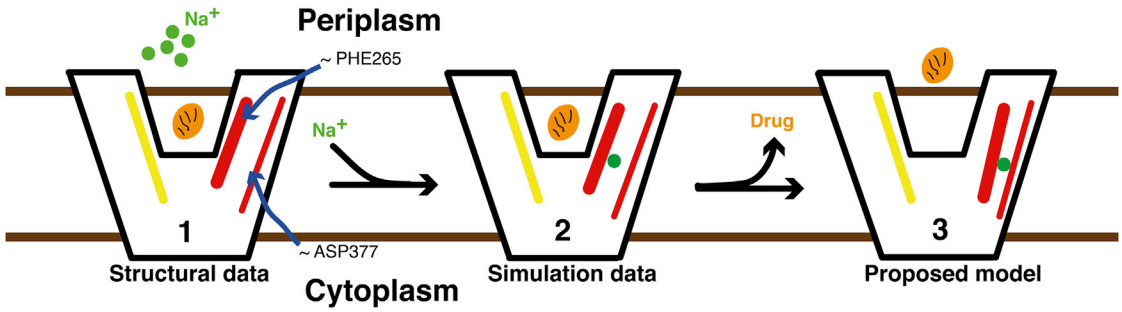

FIGURE 6 Schematic representation of the proposed mechanism of action of the outward-facing state. Na^+ ions (represented by *green spheres*) enter the protein from the extracellular side (state 1). Once the Na^+ ion is in the cation-binding site, ASP-377 binds to the Na^+ ion (state 2). This results in disruption of the interaction between residues PHE-265 with the drug molecule (*orange ellipsoid*), triggering the extrusion of the drug into the periplasm (state 3). In this mechanism, the x-ray structure of NorM-NG (PDB code 4HUK) represents state 1, state 2 is observed from MD simulations, and state 3 is hypothesized. The brown lines indicate the lipid headgroup region of the bilayer. The yellow line represents TM1 and TM2. The thick red line represents TM7 and TM8 and the thin red line represents TM10. The blue arrows indicate the approximate position of the amino acid residues PHE-265 and ASP-377. To see this figure in color, go online.

11. He, X., P. Szewczyk, …, G. Chang. 2010. Structure of a cation-bound multidrug and toxic compound extrusion transporter. *Nature.* 467: 991–994.

12. Morita, Y., A. Kataoka, …, T. Tsuchiya. 2000. NorM of *Vibrio parahaemolyticus* is an Na(+)-driven multidrug efflux pump. *J. Bacteriol.* 182:6694–6697.

13. Long, F., C. Rouquette-Loughlin, …, E. W. Yu. 2008. Functional cloning and characterization of the multidrug efflux pumps NorM from *Neisseria gonorrhoeae* and YdhE from *Escherichia coli*. *Antimicrob. Agents Chemother.* 52:3052–3060.

14. Vanni, S., P. Campomanes, …, U. Rothlisberger. 2012. Ion binding and internal hydration in the multidrug resistance secondary active transporter NorM investigated by molecular dynamics simulations. *Biochemistry.* 51:1281–1287.

15. Song, J., C. Ji, and J. Z. Zhang. 2014. Insights on Na(+) binding and conformational dynamics in multidrug and toxic compound extrusion transporter NorM. *Proteins.* 82:240–249.

16. Lu, M., J. Symersky, …, S. Koide. 2013. Structures of a Na+-coupled, substrate-bound MATE multidrug transporter. *Proc. Natl. Acad. Sci. USA.* 110:2099–2104.

17. Malde, A. K., L. Zuo, …, A. E. Mark. 2011. An automated force field topology builder (ATB) and repository: version 1.0. *J. Chem. Theory Comput.* 7:4026–4037.

18. Maarten, G., M. H. Wolf, …, G. Groenhof. 2010. g membed: efficient insertion of a membrane protein into an equilibrated lipid bilayer with minimal perturbation. *J. Comput. Chem.* 31:2169–2174.

19. van der Spoel, D., E. Lindahl, …, H. J. C. Berendsen. 2005. GROMACS: fast, flexible, and free. *J. Comput. Chem.* 26:1701–1718.

20. Berendsen, H. J. C., D. Vanderspoel, and R. Vandrunen. 1995. Gromacs: a message-passing parallel molecular-dynamics implementation. *Comput. Phys. Commun.* 91:43–56.

21. Hess, B., C. Kutzner, …, E. Lindahl. 2008. GROMACS 4: algorithms for highly efficient, load-balanced, and scalable molecular simulation. *J. Chem. Theory Comput.* 4:435–447.

22. Schmid, N., A. P. Eichenberger, …, W. F. van Gunsteren. 2011. Definition and testing of the GROMOS force-field versions 54A7 and 54B7. *Eur. Biophys. J.* 40:843–856.

23. Berger, O., O. Edholm, and F. Jähnig. 1997. Molecular dynamics simulations of a fluid bilayer of dipalmitoylphosphatidylcholine at full hydration, constant pressure, and constant temperature. *Biophys. J.* 72:2002–2013.

24. Berendsen, H. J. C., J. P. M. Postma, …, J. Hermans. 1981. *In* Intermolecular Forces, B. Pollman, editor. Reidel, Dordrecht, pp. 331–342.

25. Hess, B. 2008. P-LINCS: a parallel linear constraint solver for molecular simulation. *J. Chem. Theory Comput.* 4:116–122.

26. Miyamoto, S., and P. A. Kollman. 1992. Settle—an analytical version of the SHAKE and RATTLE algorithm for rigid water models. *J. Comput. Chem.* 13:952–962.

27. Hoover, W. G. 1985. Canonical dynamics: equilibrium phase-space distributions. *Phys. Rev. A.* 31:1695–1697.

28. Parrinello, M., and A. Rahman. 1981. Polymorphic transitions in single crystals: a new molecular dynamics method. *J. Appl. Phys.* 52:7182–7190.

29. Essmann, U., L. Perera, …, L. G. Pedersen. 1995. A smooth particle mesh Ewald method. *J. Chem. Phys.* 103:8577–8593.

30. Kabsch, W., and C. Sander. 1983. Dictionary of protein secondary structure: pattern recognition of hydrogen-bonded and geometrical features. *Biopolymers.* 22:2577–2637.

31. Humphrey, W., A. Dalke, and K. Schulten. 1996. VMD: visual molecular dynamics. *J. Mol. Graph.* 14:33–38, 27–28.

32. Flyvbjerg, H., and H. G. Petersen. 1989. Error-estimates on everages of correlated data. *J. Chem. Phys.* 91:461–466.

33. Otsuka, M., M. Yasuda, …, Y. Moriyama. 2005. Identification of essential amino acid residues of the NorM Na+/multidrug antiporter in *Vibrio parahaemolyticus*. *J. Bacteriol.* 187:1552–1558.

34. Matsumoto, T., T. Kanamoto, …, Y. Moriyama. 2008. Role of glutamate residues in substrate recognition by human MATE1 polyspecific H+/organic cation exporter. *Am. J. Physiol. Cell Physiol.* 294:C1074–C1078.

35. Holdbrook, D. A., Y. M. Leung, …, S. Khalid. 2010. Stability and membrane orientation of the fukutin transmembrane domain: a combined multiscale molecular dynamics and circular dichroism study. *Biochemistry.* 49:10796–10802.

36. Piggot, T. J., D. A. Holdbrook, and S. Khalid. 2011. Electroporation of the *E. coli* and *S. aureus* membranes: molecular dynamics simulations of complex bacterial membranes. *J. Phys. Chem. B.* 115:13381–13388.

37. Goose, J. E., and M. S. P. Sansom. 2013. Reduced lateral mobility of lipids and proteins in crowded membranes. *PLOS Comput. Biol.* 9:e1003033.